Synthesis of Novel Benzofuran-Based Thiazole Hybrids and Investigation of Their Antioxidant and Anticholinesterase Activities

Betül KAYA**, Zahra MARYAM**, Nour El-Huda DAOUD***, Emine Rana BAĞCI ****, *****, Abdüllatif KARAKAYA******, Tuğba ERÇETİN******, Ulviye Acar ÇEVİK********

Synthesis of Novel Benzofuran-Based Thiazole Hybrids and Investigation of Their Antioxidant and Anticholinesterase Activities Benzofuran Temelli Yeni Tiyazol Hibritlerinin Sentezi ve Antioksidan ve Antikolinesteraz Aktivitelerinin İncelenmesi

SUMMARY

In this study, a novel series of benzofuran derivatives (2a-2k) was synthesized, and the structures of the obtained compounds were elucidated by 1H NMR, 13C NMR, and HRMS spectra. The compounds were investigated for their anticholinesterase and antioxidant potentials. The ferrous ion chelating activity of the compound 2g at 50 µM concentration was 68.25%, surpassing those of rutin and BHT (13.21% and 2.57%, respectively). Besides, according to the DPPH radical scavenging activity assay, compound 2g exhibited the most potent antioxidant activity with an IC50 value of $30.14 \pm 0.005 \,\mu\text{M}$, when compared to standard gallic acid (IC50 $29.48 \pm 0.014 \mu M$). Furthermore, compounds 2d (10.33%) and 2i(20.17%) showed the highest inhibitory activity against AChE and BChE, respectively. Compound 2i exhibits important interactions with the active site of BChE, according to the in silico molecular docking study. Also, the in silico ADMET study revealed the desirable pharmacokinetic properties of compound 2i. Therefore, compounds 2g and 2i could be deemed as promising candidates for designing dual functional antioxidant and butyrylcholinesterase inhibitors in the management of Alzheimer's disease.

Keywords: Benzofuran, Alzheimer's disease, anticholinesterase, DPPH assay, ferrous ion-chelating activity.

ÖZ

Bu çalışmada, bir seri yeni benzofuran türevi bileşik (2a-2k) sentezlenmiş ve elde edilen bileşiklerin yapıları 1H NMR, 13C NMR ve HRMS spektrumları ile aydınlatılmıştır. Bileşikler antikolinesteraz ve antioksidan potansiyelleri açısından incelenmiştir. 50 µM konsantrasyonda, 2g bileşiğinin (%68,25), demir iyonu şelatlama aktivitesinin rutin ve BHT'den (sırasıyla %13,21 ve %2,57) daha yüksek olduğu bulunmuştur. Ayrıca, DPPH radikal süpürücü aktivite deneyine göre, 2g bileşiği, referans gallik asitle (IC50= 29,48 ± 0,014 µM) karşılaştırıldığında, 30,14 ± 0,005 μM'lik bir IC50 değeriyle en güçlü antioksidan aktiviteyi göstermiştir. Bunun dışında, 2d (%10,33) ve 2i (%20 , 17) bileşikleri, sırasıyla AChE ve BChE'ye karşı en yüksek inhibitör aktiviteyi göstermiştir. Bileşik 2i, in silico moleküler yerleştirme çalışmasına göre BChE'nin aktif bölgesiyle önemli etkileşimler sergilemiştir. Ayrıca, in silico ADMET çalışması, bileşik 2i'nin istenen farmakokinetik özelliklerini ortaya koymuştur. Bu nedenle, 2g ve 2i bileşikleri, Alzheimer hastalığının yönetiminde çift fonksiyonlu antioksidan ve bütirilkolinesteraz inhibitörlerinin tasarlanması için umut verici adaylar olarak öne çıkmıştır.

Anahtar Kelimeler: Benzofuran, Alzheimer hastalığı, antikolinesteraz, DPPH testi, demir iyon şelatlama aktivitesi.

Recieved: 17.04.2025 Revised: 1.09.2025 Accepted: 9.09.2025

ORCID: 0000-0002-1713-9485 Vocational School of Health Services, Pharmacy Services, Bilecik Şeyh Edebali University 11000, Bilecik, Turkey

[&]quot;ORCID: 0000-0003-4233-727X Department of Pharmaceutical Chemistry, Faculty of Pharmacy, Anadolu University, Eskişehir 26470, Turkey.

[&]quot;ORCID: 0000-0003-1332-9609 Department of Pharmaceutical Chemistry, Graduate Education Institute, Anadolu University, Eskişehir 26470, Turkey.

[&]quot;"ORCID: 0009-0004-7452-0532 Department of Pharmaceutical Chemistry, Graduate Education Institute, Anadolu University, Eskişehir 26470, Turkey.

^{·····} ORCID: 0009-0004-7452-0532 Department of Pharmaceutical Chemistry, Faculty of Pharmacy, Afyonkarahisar Health Sciences University, Afyonkarahisar 03030, Turkey

[&]quot;"" ORCID: 0009-0003-9619-6705 Department of Pharmaceutical Chemistry, Graduate Education Institute, Anadolu University, Eskişehir 26470, Turkey.

[&]quot;"" ORCID: 0009-0003-9619-6705 Department of Pharmaceutical Chemistry, Faculty of Pharmacy, Zonguldak Bulent Ecevit University, 67600 Zonguldak, Turkey

ORCID: 0000-0001-7774-7266 Department of Pharmacognosy, Faculty of Pharmacy, Eastern Mediterranean University, Via Mersin 10, TR-99628 Famagusta, North Cyprus, Turkey ORCID: 0000-0003-1879-1034 Department of Pharmaceutical Chemistry, Faculty of Pharmacy, Anadolu University, Eskişehir 26470, Turkey.

[°] Corresponding Author;Betül KAYA E-mail: betul.kaya@bilecik.edu.tr

INTRODUCTION

Alzheimer's disease (AD) is a chronic condition characterized by the irreversible degeneration of neurons in the central nervous system (CNS), resulting in progressive impairment of memory, reduced ability to speak and understand language, and other cognitive impairments that eventually lead to death (Goyal et al., 2017). There are an estimated 50 million cases of AD worldwide, according to the World Alzheimer's Disease Report, and this figure is expected to increase rapidly to 152 million cases by 2050 (Zong et al.,2023). Neurofibrillary tangles (NFT) and extracellular β -amyloid plaques (A β) are the primary pathological features of AD (Li et al., 2018). The decreased levels of cholinergic neurotransmitter, namely acetylcholine (ACh) in neural synapses, and metal dyshomeostasis linked to accelerated oxidative processes also potentiate the risk of AD. However, the exact pathogenesis of AD remains elusive, and comprehending the process of AD has been deemed essential for developing effective anti-AD drugs (Pravin and Jozwiak, 2022; Sepehri et al., 2022).

Based on the cholinergic theory, anticholinesterase inhibitors offer a solid foundation for treating AD by preserving cholinergic functionality. Anticholinesterase inhibitors perform their action by inhibiting two isoforms of human cholinesterase enzymes: acetyl cholinesterase (AChE) and butyryl cholinesterase (BChE). AChE is the primary enzyme for the disintegration of 80% of acetylcholine present in the body and is mostly found in the CNS (Marucci et al., 2021). Thus, the suppression of AChE and BChE enzymes maintains ACh level by decreasing its breakdown rate, improving short-term memory and other Alzheimer's symptoms at the cognitive level. Anticholinesterase inhibitors are considered first-line therapy for mild-to-moderate symptoms of AD. To date, four medications are approved by the FDA to treat AD symptoms, namely donepezil, memantine, rivastigmine, and galantamine (Figure 1), which are acetylcholinesterase inhibitors except memantine (Goyal et al., 2018).

$$H_3$$
CO
 H_3 CO
 H_3 CO
 H_3 CO
 H_3 CO
 H_3 CO
 H_3 CO
 H_3 CO
 H_3 CO
 H_3 CO
 H_3 CO
 H_3 CO
 H_3 CO
 H_3 CO
 H_3 CO
 H_3 CO
 H_3 CO
 H_3 CO
 H_3 CO
 H_3 CO
 H_3 CO
 H_3 CO
 H_3 CO
 H_3 CO
 H_3 CO
 H_3 CO
 H_3 CO
 H_3 CO
 H_3 CO
 H_3 CO
 H_3 CO
 H_3 CO
 H_3 CO
 H_3 CO
 H_3 CO
 H_3 CO
 H_3 CO
 H_3 CO
 H_3 CO
 H_3 CO
 H_3 CO
 H_3 CO
 H_3 CO
 H_3 CO
 H_3 CO
 H_3 CO
 H_3 CO
 H_3 CO
 H_3 CO
 H_3 CO
 H_3 CO
 H_3 CO
 H_3 CO
 H_3 CO
 H_3 CO
 H_3 CO
 H_3 CO
 H_3 CO
 H_3 CO
 H_3 CO
 H_3 CO
 H_3 CO
 H_3 CO
 H_3 CO
 H_3 CO
 H_3 CO
 H_3 CO
 H_3 CO
 H_3 CO
 H_3 CO
 H_3 CO
 H_3 CO
 H_3 CO
 H_3 CO
 H_3 CO
 H_3 CO
 H_3 CO
 H_3 CO
 H_3 CO
 H_3 CO
 H_3 CO
 H_3 CO
 H_3 CO
 H_3 CO
 H_3 CO
 H_3 CO
 H_3 CO
 H_3 CO
 H_3 CO
 H_3 CO
 H_3 CO
 H_3 CO
 H_3 CO
 H_3 CO
 H_3 CO
 H_3 CO
 H_3 CO
 H_3 CO
 H_3 CO
 H_3 CO
 H_3 CO
 H_3 CO
 H_3 CO
 H_3 CO
 H_3 CO
 H_3 CO
 H_3 CO
 H_3 CO
 H_3 CO
 H_3 CO
 H_3 CO
 H_3 CO
 H_3 CO
 H_3 CO
 H_3 CO
 H_3 CO
 H_3 CO
 H_3 CO
 H_3 CO
 H_3 CO
 H_3 CO
 H_3 CO
 H_3 CO
 H_3 CO
 H_3 CO
 H_3 CO
 H_3 CO
 H_3 CO
 H_3 CO
 H_3 CO
 H_3 CO
 H_3 CO
 H_3 CO
 H_3 CO
 H_3 CO
 H_3 CO
 H_3 CO
 H_3 CO
 H_3 CO
 H_3 CO
 H_3 CO
 H_3 CO
 H_3 CO
 H_3 CO
 H_3 CO
 H_3 CO
 H_3 CO
 H_3 CO
 H_3 CO
 H_3 CO
 H_3 CO
 H_3 CO
 H_3 CO
 H_3 CO
 H_3 CO
 H_3 CO
 H_3 CO
 H_3 CO
 H_3 CO
 H_3 CO
 H_3 CO
 H_3 CO
 H_3 CO
 H_3 CO
 H_3 CO
 H_3 CO
 H_3 CO
 H_3 CO
 H_3 CO
 H_3 CO
 H_3 CO
 H_3 CO
 H_3 CO
 H_3 CO
 H_3 CO
 H_3 CO
 H_3 CO
 H_3 CO
 H_3 CO
 H_3 CO
 H_3 CO
 H_3 CO
 H_3 CO
 H_3 CO
 H_3 CO
 H_3 CO
 H_3 CO
 H_3 CO
 H_3 CO
 H_3 CO
 H_3 CO
 H_3 CO
 H_3 CO
 H_3 CO
 H_3 CO
 H_3 CO
 H_3 CO
 H_3 CO
 H_3 CO
 H_3 CO
 H_3 CO
 H_3 CO
 H_3 CO
 H_3 CO
 H_3 CO
 H_3 CO
 H_3 CO
 H_3 CO
 H_3 CO
 H_3 CO
 H_3 CO
 H_3 CO
 H_3 CO
 H_3 CO
 H_3 CO
 H_3 CO
 H_3 CO
 H_3 CO
 H_3 CO
 H_3 CO
 H_3 CO
 H_3 CO
 H_3 CO
 H_3 CO
 H_3 CO
 H_3 CO
 H_3 CO
 H_3 CO
 H_3 CO
 H_3 CO
 H_3 CO
 H_3 CO
 H_3 CO
 H_3 CO
 H_3 CO
 H_3 CO
 H_3 CO
 H_3 CO
 H_3 CO
 H_3 CO
 H_3 CO
 H_3 CO
 H_3 CO
 H_3 CO
 H_3 CO
 H_3 CO
 H_3 CO
 H_3 CO
 H_3 CO
 H_3 CO
 H_3 CO
 H_3 CO
 H_3 CO
 H_3 CO
 H_3 CO
 H_3

Figure 1. FDA-approved drugs used in the treatment of AD.

In the field of medicinal chemistry, heterocyclic scaffolds such as benzofuran (Irfan et al., 2023b), furan (Loğoğlu et al., 2010), pyrazole (Karrouch et al., 2018), oxadiazole (Irfan et al., 2023a), and thiazole (Ripain and Ngah, 2021) have garnered considerable

attention because of their remarkable biological applications. Benzofuran, in particular, has drawn great attention and is considered a valuable class and a key structural motif in the field of drug discovery. Based on their structure, benzofuran-containing

molecules have a variety of pharmacological actions, including anti-hyperlipidemic, anti-inflammatory, analgesic, antiviral, antibacterial, anticancer, and anti-Alzheimer's properties (Arce-Ramos et al., 2023; Dawood 2019; Patel et al., 2024; Sahu et al., 2024). Thus, the benzofuran chemical core has been the subject of numerous synthetic investigations. Recently, it has been revealed that benzofuran-containing heterocyclic scaffolds (Figure 2), including hydroxypyridinone-containing benzofuran (compound 7d), coumarin-linked benzofuran (compound 9j), tacrine-derived benzofuran (compound 15), and benzofuran-based benzyl pyridinium (compound 5e) are powerful AChE inhibitors (Baharloo et al., 2015; Hiremathad et al.,

2018a; Hiremathad et al., 2018b; Fancellu et al., 2020). Besides, the benzofuran scaffold may be considered as a bioisosteric alternative to the indanone ring present in donepezil and galantamine, and benzofuran derivatives, therefore, have been explored as anti-Alzheimer's disease agents due to the structural variety while maintaining the possibility of interaction with the cholinesterase active site (Fancellu et al., 2020; Gebeş-Alperen et al., 2025). Moreover, thiazole scaffolds have appeared as prominent pharmacophores in medicinal chemistry for their numerous outstanding therapeutic efficacies, including anti-acetylcholinesterase efficacy (Haroon et al., 2021; Jehangir et al., 2024; Saglik et al., 2020; Xu et al., 2020).

$$\begin{array}{c} \text{BzO} & \text{CH}_3 \\ \text{O} & \text{O} & \text{CH}_3 \\ \text{compound 7d} & \text{compound 9j} \\ \\ \text{CI} & \text{NH} & \text{NH} & \text{O} \\ \text{CI} & \text{Supposed 15} \\ \text{compound 15} & \text{compound 5e} \\ \end{array}$$

Figure 2. Some examples of the benzofuran-based compounds that have been reported to have AChE inhibitory activity

In this study, a novel series of benzofuran derivatives including a thiazole ring was synthesized, characterized through NMR and HRMS techniques, and tested for their AChE/BChE inhibitory activities and antioxidant effects.

RESULTS AND DISCUSSION

Chemistry

In this study, new benzofuran derivatives 2a-2k were yielded as outlined in Scheme 1. The target compounds were obtained via a two-step synthetic

procedure. Firstly, 6-hydroxybenzofuran-3(2*H*)-one was reacted with thiosemicarbazone under reflux in ethanol to synthesize the corresponding thiosemicarbazone (1). Secondly, the reaction of compound 1 with appropriate 2-bromoacetophenone derivatives in ethanol afforded the title compounds 2a-2k. The structures of synthesized compounds were elucidated through NMR and HRMS techniques.

In the ¹H NMR spectra of the compounds, -CH₂ protons belonging to the benzofuran ring were

observed at between 4.68-4.71 ppm as singlets. In the 13 C NMR spectra of compounds, the peak due to -CH $_2$ carbons was obtained at between 56.24 and 56.52 ppm. The signals of all other aliphatic and

aromatic protons and carbons were detected in their expected regions. HRMS spectra corresponded with the proposed structures for all compounds.

Comp.	$R_{_1}$	$R_{_2}$	$R_{_3}$	Comp.	R ₁	$R_{_2}$	R ₃
2a	-NO ₂	-H	-H	2g	-Cl	-Cl	-H
2b	-OCH ₃	-H	-H	2h	-F	-H	-F
2c	-CN	-H	-H	2i	-Cl	-H	-H
2d	-F	-H	-H	2j	-H	-H	-H
2e	-Br	-H	-H	2k	-H	-NO ₂	-H
2f	-CH ₃	-H	-H				

Scheme 1. The synthetic route and substituents of the title compounds **2a-2k.** Reagents and conditions: first step: thiosemicarbazide, EtOH, reflux, 3h; second step: appropriate 2-bromoacetophenone derivative, EtOH, reflux, 4h.

AChE and BChE inhibitory activity

The inhibitory activity of compounds 2a-2k was measured against AChE and BchE using Galantamine hydrobromide as a reference, and the results were depicted in Table 1. Compounds 2c and 2d were detected as the most potent compounds, displaying 10.33 and 10.13% inhibition against AChE, respectively. The compounds represented a better inhibitory profile against BChE than AChE. Compounds 2i and

2h were found to be the most effective agents against BChE, with the inhibition percentage of 20.17% and 16.67%, respectively. This differential behavior can be explained by better binding of disubstituted groups with BChE. Based on these results, it can be suggested that *para*-cyano and *para*-fluoro groups are favorable for AChE inhibition, while *para*-chloro and *ortho*, *para*-difluoro substituents are suitable for BChE inhibitory activity.

Table 1. The inhibitory effects (%) of the compounds 2a-2k against cholinesterases at 50 μM reaction concentrations.

Compound	AChE	BChE
2a	NA	NA
2b	NA	NA
2c	10.13 ± 0.002	8.37 ± 0.003
2d	10.33 ± 0.008	4.94 ± 0.007
2e	NA	NA
2f	1.43 ± 0.001	5.67 ± 0.002
2g	NA	2.14 ± 0.001
2h	NA	16.67 ± 0.009
2i	2.05 ± 0.001	20.17 ± 0.011
2j	6.81 ± 0.004	2.78 ± 0.001
2k	3.76 ± 0.001	7.64 ± 0.003
Gal HBr 50 μM	97.89 ± 0.01	62.48 ± 0.01

*NA: not-active

Antioxidant Activity

The antioxidant potential of synthesized compounds **2a-2k** was measured using DPPH free radical-scavenging and ferrous ion chelating activities (Table 2). In the DPPH test, compounds **2b**, **2g**, and **2k** showed promising antioxidant activities with IC₅₀ values of 44.17 \pm 0.012 μ M, 48.11 \pm 0.014 μ M, 30.14 \pm 0.005 μ M, and 44.28 \pm 0.009 μ M, respectively. In particular, compound **2g**, with *meta*, *para*-dichloro substituent on the phenyl, ring exerted approximately equal antioxidant activity to the reference drug gallic acid. It can be suggested that *para*-methoxy (**2b**),

para-fluoro (2d), meta, para-dichloro (2g), and metanitro (2k) groups have a positive contribution to the DPPH radical-scavenging activity. According to the ferrous ion chelating potential of the compounds 2a-2k, compounds 2c, 2d, 2i, and 2j were found to have better chelating capacity (5.34%, 3.99%, 4.70% and 5.08%, respectively, at 50 μM) than BHT (2.57% at 50 μM). It can be claimed that para-cyano (2c), parafluoro (2d), and para-chloro (2i) substituents on the phenyl ring and also no substitution on the phenyl ring, have a positive contribution to the ferric ion chelating activity.

Table 2. The effects of the synthesized compounds 2a-2k at $50 \,\mu\text{M}$ and references on ferric ion chelating and DPPH free radical-scavenging (inhibition % \pm S.E.M).

Compound	DPPH	ION CHELATING
2a	6.68 ± 0.009	NA
2b	58.09 ± 0.006	2.08 ± 0.008
2c	38.98 ± 0.031	5.34 ± 0.012
2d	53.14 ± 0.042	3.99 ± 0.005
2e	37.47 ± 0.012	1.78 ± 0.003
2f	46.56 ± 0.005	1.79 ± 0.001
2g	68.25 ± 0.023	1.66 ± 0.019
2h	46.46 ± 0.008	1.38 ± 0.008
2i	46.41 ± 0.002	4.70 ± 0.012
2j	5.68 ± 0.003	5.08 ± 0.009
2k	57.50 ± 0.001	2.41 ± 0.006
RUTIN 50 μM	-	13.21 ± 0.007
RUTIN 100 μM	-	28.14± 0.011
ΒΗΤ 50 μΜ	-	2.57 ± 0.004
ΒΗΤ 100 μΜ	-	7.06 ± 0.009
Gallic Acid	70.29 ± 0.005	

^{*}NA: not-active

Table 3. DPPH free radical-scavenging activity of the synthesized compounds **2a-2k** and gallic acid (IC₅₀)

Compound	IC ₅₀ (μM)	Compound	IC_{50} (μM)
2a	$>60~\mu\mathrm{M}$	2g	30.14 ± 0.005
2b	44.17 ± 0.012	2h	53.29 ± 0.011
2c	$>60~\mu\mathrm{M}$	2i	53.31 ± 0.015
2d	48.11 ± 0.014	2j	$>60~\mu\mathrm{M}$
2e	$>60~\mu M$	2k	44.28 ± 0.009
2f	53.21 ± 0.008	Gallic Acid	29.48 ± 0.014

Molecular Docking Study and ADMET

This molecular docking illustrates how compound **2i** binds to the active site of BChE, providing detailed insights into its binding interactions and potential efficacy. During the preparation step, compound **2i**,

a proton was transferred between the nitrogen atom of hydrazine and the thiazole ring due to the selected pH range (5-9) and different pKa values for each of them; N (hydrazine) 1.17 and N (thiazole) 9.63 (see Figure 3).

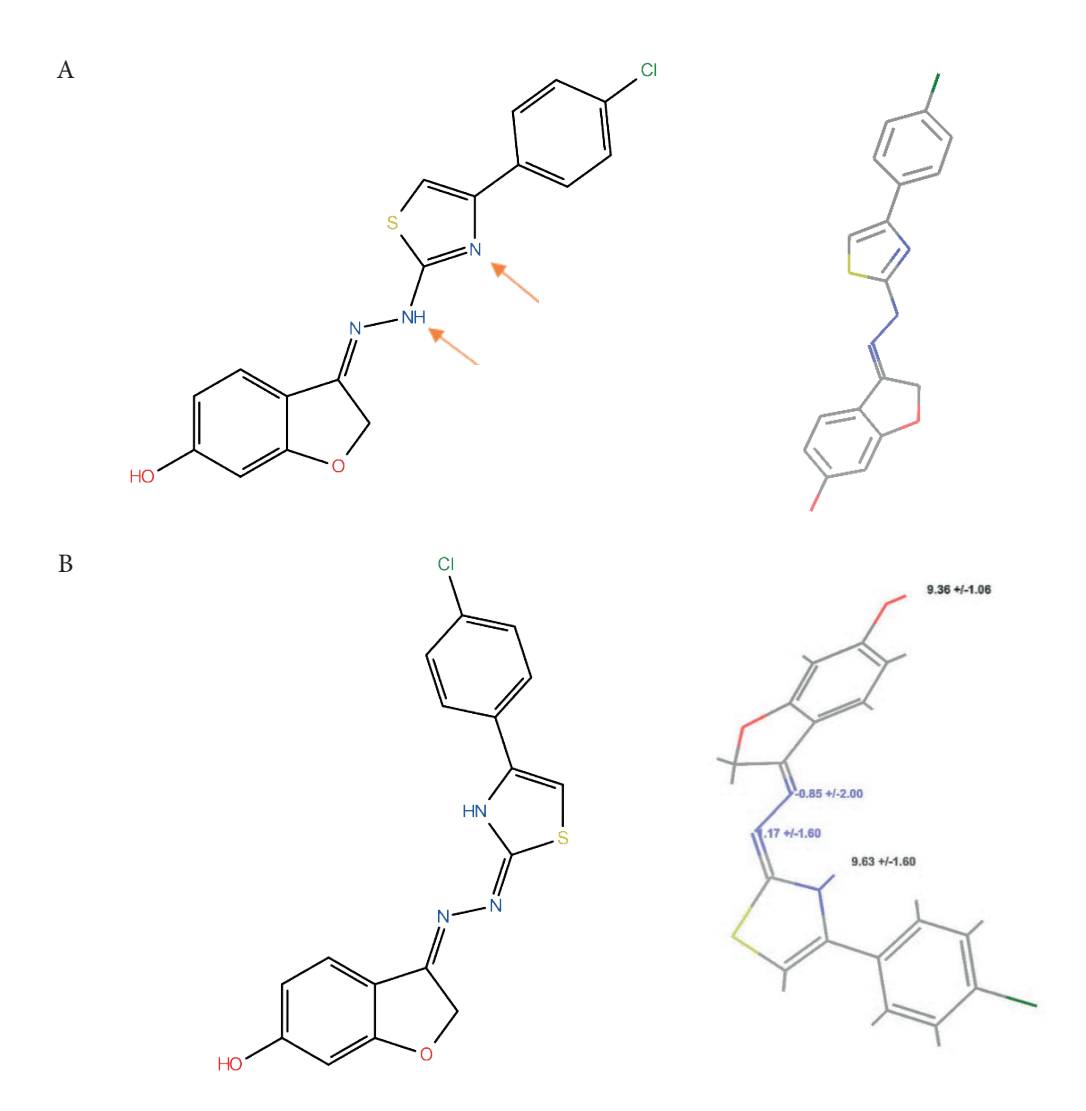


Figure 3. Show compound **2i**, (A) before preparation, (B) after preparation step for docking, and the predicted pKa for each atom in compound **2i**, which justifies the different generated forms for the compound before and after preparation on the pH range (5-9).

The docking results are presented in Table 4. The docking scores (glide gscore) for both SP and XP docking modes are -7.392 and -7.279 Kcal/mol, respectively. Protonated and deprotonated forms.

However, the docking gscore for the co-crystalized ligand (Tacrine) was lower in the XP mode (-6.301 Kcal/mol), which indicates that our compound **2i** binds more effectively to the BChE.

Table 4. The computational results from	docking compound	2i in BChE enzyme	(4BDS) (Kcal/mol);
different docking scores with the glide property	у.		

Docking Mode	Standard precision mode (SP)	Extra precision mode (XP)
Docking score	-7.392	-7.279
Glide ligand efficiency	-0.308	-0.303
Glide gscore	-7.392	-7.279
Glide energy	-46.888	-41.624

The binding correspondence of BChE with compound 2i (Figure 4) is instituted by two bond types: the hydrogen bond, which is the stronger, and the Pi-Pi stacking bond, which is the weaker. The hydrogen bond is suggested to be a crucial aid in stabilizing the binding of our compound with the BChE binding pocket. The stronger bond type was found between the phenolic OH group of our

compound (2i) with Tyr 128 and Glh197 residues from the active site (two H-bonds). The weaker one formed between the hydrophobic parts of the benzene rings and the thiazole ring from our compound with Trp82, Tyr332, and Phe329 residues from the active site; formed five Pi-Pi stacking bonds. The calculated glide gscore is -7.279 Kcal/mol.

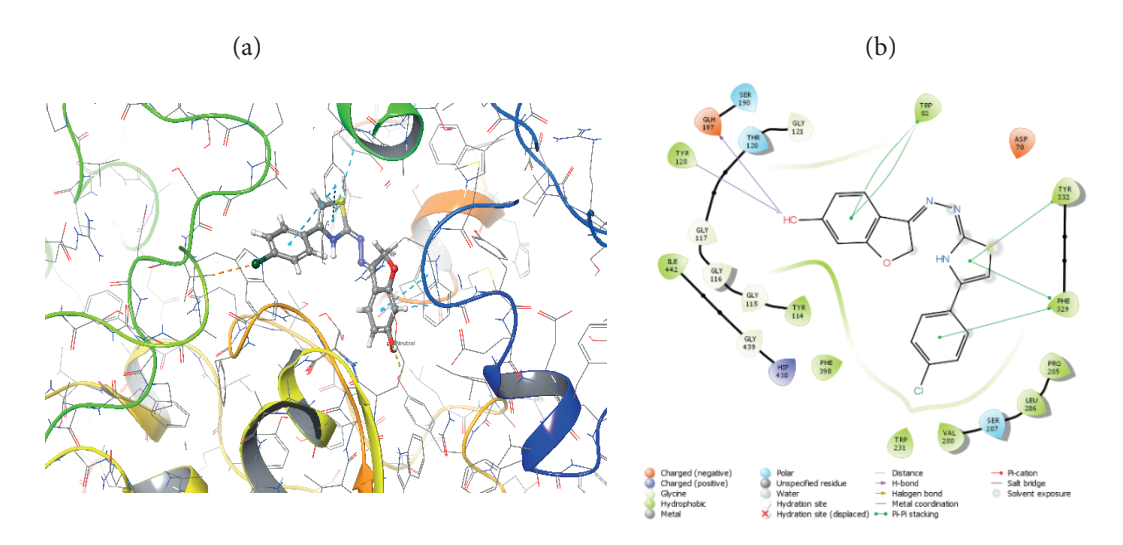


Figure 4. (a) 3D (b) 2D binding interactions between BChE with compound **2i** from XP mode, demonstrating hydrogen bonds with Glh197 and Tyr 128. Five pi-pi stacking with Trp82, Tyr332, and Phe329. The glide gscore is -7.279 Kcal/mol (PDB ID 4BDS).

After we evaluated the interaction of compound 2i with BChE, we need to check its toxicity and biological effects to figure out its potential use as a medicine. For that, we applied a computational ADMET study, which helped to predict how our lead compound affects human metabolism. The result of it is summarized in Table 5, which lists the computed

ADMET parameters for our compound 2i. According to the data, our compound may qualify as a drug because the values for Rule 5 (Lipinski, 2004) and 3 (Lipinski et al., 2012) are less than 3. Moreover, it predicts good oral absorption and high permeability in MDCK and Caco2 cells. While it also shows a few side effects, good safety, and drug-like properties.

Table 5. Predicted ADMET characteristics of the compound 2i.

Title	2i	Reference Range
Molecular weight (MW)	357.814	130-725
dipole	4.892	1.0-12.5
SASA	602.208	300-1000
FOSA	53.934	0-750
FISA	80.032	7–330
PISA	344.502	0-450
WPSA	123.741	0-175
Volume (A³)	1024.594	500-2000
Hydrogen bond donor (HBD)	2	0-6
Hydrogen bond acceptor (HBA)	3.5	2.0-20.0
Glob (Sphere = 1)	0.8161812	0.75-0.95
QPlogPC16	11.99	4.0-18.0
QPlogPoct	17.476	8.0-35.0
QPlogPw	9.814	4.0-45.0
Predicted octanol/water	4.361	-2.0-6.5
partition coefficient (QPlogPo/w)		-2.0-0.3
QPlogS	-5.866	-6.5-0.5
CIQPlogS	-6.109	-6.5-0.5
Predicted ${\rm IC}_{\rm 50}$ value for blockage of HERG K+ channels (QPlog HERG)	-6.149	Concern if it is below -5
Predicted Caco2 cell permeability (QPP Caco) (nm/sec)	1725.676	Less than 25 is poor More than 500 is great
Predicted brain/blood partition coefficient (QPlogBB)	-0.115	-3.0-1.2
Predicted MDCK cell permeability (QPPMDCK) (nm/sec)	4249.394	Less than 25 is poor More than 500 is great
Prediction of binding to human serum albumin (QPlogKhsa)	0.516	-1.5-1.5
Oral Absorption (for Human)	3	-
Human Oral Absorption as %	100	Less than 25% is poor More than 80% is high
PSA	64.89	7–200
Rule 5	0	In max of 5
Rule 3	1	In max of 3
Jm	0.016	-

MATERIAL AND METHOD

Chemistry

All starting materials and chemicals used in the synthetic route were supplied by commercial suppliers. Melting points were determined using the MP90 digital melting point apparatus (Mettler Toledo, OH, USA) and were uncorrected. ¹H-NMR and ¹³C-NMR spectra were recorded through a NMR spectrometer (Bruker, Billerica, MA, USA) in DMSO-d₆. HRMS spectra were recorded on a LCMS-IT-TOF system (Shimadzu, Kyoto, Japan). Thin Layer Chromatography (TLC) using Silica Gel 60 F254 TLC plates (Merck KGaA, Darmstadt, Germany) was performed to monitor the progress of the chemical reactions.

Synthesis of 2-(6-hydroxybenzofuran-3(2*H*)-ylidene)methyl-hydrazine-1-carbothioamide (1) (CAS Number: 1535209-86-9): Ethanol (100 mL) was used to dissolve thiosemicarbazide (2.89 g, 0.032 mol) and 6-hydroxybenzofuran-3(2*H*)-one (4.8 g, 0.032 mol). The mixture was refluxed for three hours. After completion of the reaction, the reaction mixture was chilled in an ice bath, and the precipitated product was filtered and crystallized from ethanol (Laczkowski et al., 2013).

Synthesis of target compounds (2a-2k): The appropriate 2-bromoacetophenone derivative (2.5 mmol) and 2-(6-hydroxybenzofuran-3(2*H*)-ylidene) methyl-hydrazine-1-carbothioamide (1) (2.5 mmol) were dissolved in ethanol (50 mL). The mixture was refluxed for four hours. After TLC screening, the mixture was cooled in an ice bath, and the precipitated product was filtered and crystallized from ethanol.

3-(2-(4-(4-Nitrophenyl) thiazol-2-yl) hydrazineylidene)-2,3-dihydrobenzofuran-6-ol (2a): Yield: 78 %, M.P.= 155.4 °C. ¹H-NMR (400 MHz, DMSO-d₆): δ: 4.70 (2H, s, CH₂), 6.51 (1H, s, Aromatic CH), 6.58 (1H, d, J= 8.44 Hz, Aromatic CH), 7.31 (1H, br.s, Aromatic CH), 7.45 (1H, d, J= 8.96 Hz, Aromatic CH), 8.02 (2H, d, J= 7.88 Hz, Aromatic CH), 8.27 (2H, d, J= 8.00 Hz, Aromatic CH). 13 C-NMR (100 MHz, DMSO-d₆): δ= 56.48, 112.23, 113.40, 124.27, 124.54, 125.49, 126.94, 130.04, 139.18, 145.00, 150.08, 155.80, 167.18, 176.05, 197.25. HRMS (m/z): [M+H]+ calcd for C₁₂H₁₂N₄O₄S: 369.0652; found: 369.0651.

3-(2-(4-(4-Methoxyphenyl)thiazol-2-yl) hydrazineylidene)-2,3-dihydrobenzofuran-6-ol (2b): Yield: 76 %, M.P.= 112.9 °C. ¹H-NMR (400 MHz, DMSO- 4 0: δ: 3.82 (3H, s, -OCH 3), 4.69 (2H, s, CH 2 0), 6.53 (1H, s, Aromatic CH), 6.59 (1H, d, 4 1 = 8.48 Hz, Aromatic CH), 7.01-7.03 (2H, m, Aromatic CH), 7.44 (1H, d, 4 1 = 8.28 Hz, Aromatic CH), 7.67 (1H, d, 4 1 = 7.92 Hz, Aromatic CH), 7.91 (2H, d, 4 1 = 7.60 Hz, Aromatic CH). 13 C-NMR (100 MHz, DMSO- 4 6): δ= 55.78, 56.52, 98.08, 100.94, 112.58, 114.15, 115.07, 125.42, 127.63, 130.68, 160.60, 163.74, 167.16, 170.76, 176.03,

197.18. HRMS (m/z): [M+H]⁺ calcd for C₁₈H₁₅N₃O₃S: 354.0907; found: 354.0901.

3-(2-(4-(4-Cyanophenyl)thiazol-2-yl) hydrazineylidene)-2,3-dihydrobenzofuran-6-ol (2c): Yield: 69 %, M.P.= 129.4 °C. ¹H-NMR (400 MHz, DMSO-d₆): δ: 4.70 (2H, s, CH₂), 6.51 (1H, s, Aromatic CH), 6.58 (1H, d, J= 8.52 Hz, Aromatic CH), 7.45 (2H, d, J= 8.36 Hz, Aromatic CH), 7.92-7.94 (2H, m, Aromatic CH), 8.01-8.04 (2H, m, Aromatic CH). 13 C-NMR (100 MHz, DMSO-d₆): δ= 56.48, 98.76, 112.24, 113.39, 125.48, 126.58, 126.77, 129.23, 132.64, 132.84, 133.22, 145.27, 158.66, 167.19, 176.04, 197.26. HRMS (m/z): [M+H]⁺ calcd for C₁₈H₁₂N₄O₂S: 349.0754; found: 349.0746.

3-(2-(4-(4-Fluorophenyl) thiazol-2-yl) hydrazineylidene)-2,3-dihydrobenzofuran-6-ol (2d): Yield: 77 %, M.P.= 91.2 °C. ¹H-NMR (400 MHz, DMSO-d₆): δ: 4.70 (2H, s, CH₂), 6.52 (1H, s, Aromatic CH), 6.58 (1H, d, J= 8.24 Hz, Aromatic CH), 7.45 (2H, d, J= 8.44 Hz, Aromatic CH), 7.80-7.82 (2H, m, Aromatic CH), 8.04-8.05 (2H, m, Aromatic CH). 13 C-NMR (100 MHz, DMSO-d₆): δ= 56.48, 98.76, 112.24, 113.40, 116.01, 116.35 (d, J= 23.8 Hz), 125.49, 128.61, 131.67, 132.28 (d, J= 9.4 Hz), 141.86, 150.26, 167.19, 176.05, 197.27. HRMS (m/z): [M+H]⁺ calcd for C₁₇H₁₂N₃O₂FS: 342.0707; found: 342.0708.

3-(2-(4-(4-Bromophenyl) thiazol-2-yl) hydrazineylidene)-2,3-dihydrobenzofuran-6-ol (2e): Yield: 75 %, M.P.= 100.5 °C. ¹H-NMR (400 MHz, DMSO-d₆): δ: 4.68 (2H, s, CH₂), 6.36 (1H, s, Aromatic CH), 6.49-6.57 (2H, m, Aromatic CH), 7.43 (1H, s, Aromatic CH), 7.63-7.88 (4H, m, Aromatic CH). ¹³C-NMR (100 MHz, DMSO-d₆): δ= 56.24, 104.08, 112.49, 113.41, 120.71, 122.74, 123.66, 125.32, 130.68, 132.34, 141.39, 148.78, 168.08, 176.21, 197.45. HRMS (m/z): [M+H]⁺ calcd for $C_{17}H_{12}N_3O_2SBr$: 401.9906; found: 401.9913.

3-(2-(4-(4-Methylphenyl)thiazol-2-yl) hydrazineylidene)-2,3-dihydrobenzofuran-6-ol (2f): Yield: 79 %, M.P.= 98.7 °C. ¹H-NMR (400 MHz, DMSO-d_s): δ: 2.32 (3H, s, CH₃), 4.71 (2H, s, CH₂), 6.38 (1H, s, Aromatic CH), 6.59 (2H, d, J= 8.28 Hz, Aromatic CH), 7.46 (1H, d, J= 8.20 Hz, Aromatic CH), 7.45-7.47 (1H, m, Aromatic CH), 7.63 (2H, br.s, Aromatic CH), 7.85 (2H, br.s, Aromatic CH). 13 C-NMR (100 MHz, DMSO-d₆): δ = 21.30, 56.48, 102.33, 112.25, 113.40, 125.48, 126.14, 128.73, 129.66, 130.03, 143.98, 150.63, 167.20, 170.67, 176.05, 197.26. HRMS (m/z): [M+H]⁺ calcd for $C_{18}H_{15}N_3O_2S$: 338.0958; found: 338.0968.

3-(2-(4-(3,4-Dichlorophenyl)thiazol-2-yl) hydrazineylidene)-2,3-dihydrobenzofuran-6-ol (2g): Yield: 70 %, M.P.= 116.6 °C. ¹H-NMR (400 MHz, DMSO-d₆): δ: 4.70 (2H, s, CH₂), 6.51 (1H, s, Aromatic CH), 6.58 (1H, d, J= 8.44 Hz, Aromatic CH), 7.45 (2H, d, J= 8.04 Hz, Aromatic CH), 7.90 (1H, d, J= 8.32 Hz, Aromatic CH), 8.03 (1H, s, Aromatic CH), 8.11-8.13 (1H, m, Aromatic CH). ¹³C-NMR (100 MHz, DMSO-d₆): δ= 56.48, 98.76, 102.86, 112.23, 113.41, 125.49, 126.20, 127.82, 128.65, 130.56, 131.35, 131.51, 131.81, 148.78, 167.18, 176.05, 197.25. HRMS (m/z): [M+H]⁺ calcd for C₁₇H₁₁N₃O₂SCl₂: 392.0022; found: 392.0027.

3-(2-(4-(2,4-Diflorophenyl)thiazol-2-yl) hydrazineylidene)-2,3-dihydrobenzofuran-6-ol (2h): Yield: 73 %, M.P.= 117.8 °C. ¹H-NMR (400 MHz, DMSO-d₆): δ : 4.69 (2H, s, CH₂), 6.56 (1H, s, Aromatic CH), 6.61 (1H, d, J= 8.24 Hz, Aromatic CH), 7.12 (1H, s, Aromatic CH), 7.24 (1H, s, Aromatic CH), 7.37 (1H, s, Aromatic CH), 7.44 (1H, d, J= 8.36 Hz, Aromatic CH), 7.50 (1H, s, Aromatic CH). ¹³C-NMR (100 MHz, DMSO-d₆): δ = 56.47, 98.77, 105.54, 112.31, 113.30, 125.40, 130.84 and 130.96 (dd, J₁= 3.7 Hz, J₂= 11.6 Hz), 132.17, 148.16, 162.25, 165.34, 167.37, 170.03, 176.04, 197.25. HRMS (m/z): [M+H]⁺ calcd for C₁₇H₁₁N₃O, F,S: 360.0613; found: 360.0612.

3-(2-(4-(4-Chlorophenyl)thiazol-2-yl) hydrazineylidene)-2,3-dihydrobenzofuran-6-ol (2i): Yield: 77 %, M.P.= 123.9 °C. ¹H-NMR (400 MHz, DMSO-d₆): δ: 4.70 (2H, s, CH₂), 6.51 (1H, s, Aromatic CH), 6.58 (1H, d, J= 8.28 Hz, Aromatic

CH), 7.44-7.47 (2H, m, Aromatic CH), 7.55-7.60 (3H, m, Aromatic CH), 7.76 (1H, d, J= 7.08 Hz, Aromatic CH). 13 C-NMR (100 MHz, DMSO-d₆): δ = 98.75, 112.23, 113.39, 125.47, 128.04, 128.80, 129.23, 129.46, 129.57, 130.53, 133.17, 167.19, 176.05, 197.26. HRMS (m/z): [M+H]⁺ calcd for $C_{17}H_{12}N_3O_2$ SCl: 358.0412; found: 358.0419.

3-(2-(4-Phenyl)thiazol-2-yl)hydrazineylidene)-2,3-dihydrobenzofuran-6-ol (2j): Yield: 78 %, M.P.= $129.8\,^{\circ}\text{C}$. ^{1}H -NMR (400 MHz, DMSO-d_o): δ : 4.71 (2H, s, CH₂), 6.43 (1H, m, Aromatic CH), 6.53-6.59 (2H, m, Aromatic CH), 7.10 (2H, s, Aromatic CH), 7.25 (3H, s, Aromatic CH), 7.92 (1H, s, Aromatic CH). ^{13}C -NMR (100 MHz, DMSO-d_o): δ = 56.49, 98.78, 112.25, 113.40, 125.46, 126.27, 127.46, 128.58, 128.82, 129.12, 129.48, 131.92, 167.20, 176.05, 197.23. HRMS (m/z): [M+H]⁺ calcd for $C_{17}H_{13}N_3O_2S$: 324.0801; found: 324.0809.

3-(2-(4-(3-Nitrophenyl) thiazol-2-yl) hydrazineylidene)-2,3-dihydrobenzofuran-6-ol (2k): Yield: 76 %, M.P.= 146.4 °C. ¹H-NMR (400 MHz, DMSO-d₆): δ: 4.70 (2H, s, CH₂), 6.51 (1H, s, Aromatic CH), 6.58 (1H, d, J= 8.48 Hz, Aromatic CH), 7.45 (2H, d, J= 7.80 Hz, Aromatic CH), 7.71-7.73 (2H, m, Aromatic CH), 8.20 (2H, br.s., Aromatic CH). 13 C-NMR (100 MHz, DMSO-d₆): δ= 56.48, 98.75, 112.23, 113.40, 120.45, 122.72, 123.25, 125.48, 130.56, 130.72, 132.01, 132.34, 148.53, 148.73, 167.18, 176.04, 197.24. HRMS (m/z): [M+H]+ calcd for C_{17} H₁₂N₄O₄S: 369.0652; found: 369.0658.

Determination of AChE and BChE Inhibitory Activities

The ChE inhibitory activity of the synthesized compounds was determined using an Ellman-modified spectrophotometric technique, as described in our previous studies (Karakaya et al., 2023a; Kaya et al., 2024; Karakaya et al., 2024). Donepezil hydrochloride (Sigma-Aldrich, USA) was employed as the reference drug.

Determination of Antioxidant Activity

Ferrous ion-chelating effect

The ferrous ion-chelating effect of all compounds and references was evaluated through the method reported by Chua et al., as described in our previous studies (Karakaya et al., 2023b; Karakaya et al., 2024; Kaya et al., 2024). BHT and rutin were employed as standard compounds.

DPPH Radical Scavenging Activity

The 2,2-diphenyl-1-picrylhydrazyl (DPPH) radical scavenging activity of the compounds was determined via Blois's UV technique, as described in our previous studies (Karakaya et al., 2023b; Karakaya et al., 2024; Kaya et al., 2024). Gallic acid was used as the standard compound.

Molecular Docking Study

To design effective AChE inhibitors and or BChE, ligands must target both the peripheral anionic site (PAS) and catalytic anionic site (CAS), and maximize inhibition (Ghanei-Nasab et al., 2016; Kuzu et al., 2024). Potent AChE inhibitors often include aromatic groups to bind PAS and basic-centered groups to interact with CAS; for instance, donepezil demonstrates high inhibition by binding both sites (Ferreira et al., 2021).

The AChE active site, measuring approximately 20 Å deep and 5 Å wide, includes essential residues like Tyr70, Asp72, Tyr121, Trp279, and Tyr334 for structural integrity. The deeper CAS contains His440, Glu327, Ser200, and Trp84. Similarly, BChE has a comparable active site structure, with a catalytic triad of Ser198, His438, and Glu325, as well as CAS residues Glu197, Trp231, and Phe329, and PAS residues Asp70 and Tyr332, forming a wider binding pocket (Kuzu et al., 2024).

Successful inhibition relies on ligand interactions with these residues to effectively block cholinesterase activity (Kuzu et al., 2024). Molecular docking, a rapid, cost-effective modeling technique, evaluates these atomic interactions between small molecules and receptors, supporting drug discovery efforts (Agarwal and Mehrotra, 2016; Meng et al., 2011).

In our study, we conducted docking analyses on BChE (PDB ID: 4BDS) (Kryger et al., 1999; Nachon et al., 2013) using Maestro v12.8.117 from Schrödinger Suite 2021-2 (Schrödinger, 2021a). These specific crystal structures, selected for their biological relevance (Kuzu et al., 2024), were analyzed across a pH range of 5-9, aligning with AChE's active pH range of 7.5-8.0 (Tran-Minh et al., 1999). We developed our methodology based on Kuzu group (Kuzu et al., 2024) and Kaya group (Kaya et al., 2025) methods in protein selection (precision and relevance) and software choice. We conducted this in-silico analysis to validate our in-vitro findings regarding the compound 2i, which is identified as the most effective BChE inhibitor among others. Our objective is to illustrate its docking behavior within the active site of BChE, providing detailed insights into its binding interactions and potential efficacy.

Preparation of the compound 2i

We sketched compound 2i in Maestro and prepared for docking with the LigPrep tool (Schrödinger, 2021b) Through that, it created all stereoisomers and tautomers for the most stable conformers (32 in max) with its ionization state at neutral pH (7.0±2.0); here we applied Epik to calculate charge for ionized atoms.

Protein structure preparation

The protein structures (4BDS) were prepared for docking using the Schrodinger Impeded Protein Preparation tool (Schrödinger, 2021c). Through that, it inserted hydrogen and created zero bond ordering for metals, cap terminal, and generated ionic state at neutral pH (7.0±2.0) with Epik. Then we eliminated the co-crystal reagents except for the model ligand (Tacrine), and we restored the ionization states for the protein's polar residues to their original state. In addition, all water molecules were removed that literature proved not included in the complex formation (Ghanei-Nasab et al., 2016; Kuzu et al., 2024). Finally, we used the PROPKA procedure to produce hydrogens at pH 7. We minimized all proteins using the OPLS4 force field to decrease

steric clash between side chains, with a convergence of heavy atoms to an RMSD of 3 Å according to the method reported by Kuzu et al. (Kuzu et al., 2024).

Grid generation and docking protocol

Using the incorporated Schrodinger panel to create a grid (Schrödinger, 2021d) as a mandatory pre-step for docking. We created a grid box around the urease enzyme's active site, including the co-crystal ligands. It is 20°A in each dimension from the ligand's center, with 0.25 as the cutoff radius scaling and 1.0 as a factor for the van der Waals.

We then docked our compound twice using another incorporated panel for docking using GLIDE, first using standard precision (SP) mode and then using extra precision (XP) mode (Schrödinger, 2021e). Through that, we applied default settings and selected the final docked pose of each compound based on the highest Glide score.

For validation, the co-crystalized ligand (Tacrine) was re-located in the active site of BChE by applying the same docking modes. RMSD value equals 0.4171 and SP docking score equals -7.681.

ADMET

We used an incorporated Qik-prop (Schrödinger, 2021f) tool in Schrödinger to calculate and predict ADMET and physicochemical properties of our compound, including distribution, absorption, excretion, metabolism, and toxicity.

CONCLUSION

Regarding the significant role of the benzofuran moiety in AD management drugs, a novel series of benzofuran derivatives was successfully synthesized and characterized in this study. Compounds were tested for their cholinesterase inhibitory activity and antioxidant potential. The results revealed that compounds exhibited better BChE inhibition than AChE. Compound 2i showed the highest inhibitory activity against BChE. Moreover, the computational docking study showed that our lead compound 2i interacts significantly with the active site of BChE. Additionally, ADMET profiling using QikProp suggests that our

lead (2i) possesses favorable pharmacokinetic properties. Considering antioxidant activity, compound 2g showed promising DPPH scavenging and ferrous ion chelating activity. Thus, in the future, compounds 2i and 2g can serve as lead compounds for the development of new dual-targeted anti-AD agents that can serve as butyrylcholinesterase inhibitors and antioxidants.

Supporting Information Summary

In the supporting information, the researcher can view the full characterization data of compounds.

AUTHOR CONTRIBUTION STATEMENT

BK and UAÇ conceived and designed the study, BK, ZM, UAÇ, ERB and AK performed the synthesized compounds, BK and UAÇ performed the analysis of the compounds. TE performed anti-acetylcholinesterase (AChE), anti-butyrylcholinesterase (BChE) and antioxidant activities. NEHD performed the docking and ADMET studies. All authors reviewed and edited the manuscript. All authors read and approved the manuscript.

CONFLICT OF INTEREST

The authors declare that there is no conflict of interest.

REFERENCES

Agarwal, S., & Mehrotra, R. (2016). An overview of molecular docking. *JSM Chemistry*, 4(2), 1024-1028. Retrieved from https://www.jscimedcentral.com/journal-info/JSM-Chemistry

Arce-Ramos, L., Castillo, J. C., & Becerra, D. (2023). Synthesis and biological studies of benzo[b] furan derivatives: a review from 2011 to 2022. *Pharmaceuticals*, 16(9), 1265. doi: 10.3390/ph16091265

Baharloo, F., Moslemin, M. H., Nadri, H., Asadipour, A., Mahdavi, M., Emami, S., ... Foroumadi, A. (2015). Benzofuran-derived benzylpyridinium bromides as potent acetylcholinesterase inhibitors. European Journal of Medicinal Chemistry, 93, 196-201. doi: 10.1016/j.ejmech.2015.02.009

- Dawood, K. M. (2019). An update on benzofuran inhibitors: a patent review. *Expert Opinion on Therapeutic Patents*, 29, 841-870. doi: 10.1080/13543776.2019.1673727
- Fancellu, G., Chand, K., Tomás, D., Orlandini, E.,
 Piemontese, L., Silva, D. F., ... Santos, M. A. (2020).
 Novel tacrine-benzofuran hybrids as potential multi-target drug candidates for the treatment of Alzheimer's Disease. *Journal of Enzyme Inhibition and Medicinal Chemistry*, 35(1), 211-226. doi: 10.1080/14756366.2019.1689237
- Ferreira, J. P., Albuquerque, H. M., Cardoso, S. M., Silva, A. M., & Silva, V. L. (2021). Dual-target compounds for Alzheimer's disease: natural and synthetic AChE and BACE-1 dual-inhibitors and their structure-activity relationship (SAR). *European Journal of Medicinal Chemistry*, 221, 113492. doi: 10.1016/j.ejmech.2021.113492
- Gebeş-Alperen, B., Evren, A. E., Sağlik Özkan, B. N., Karaburun, A. C., & Gundogdu-Karaburun, N. (2025). Novel benzofuran-3-yl-methyl and aliphatic azacyclics: design, synthesis, and in vitro and in silico anti-Alzheimer disease activity studies. *ACS Omega*, 10(30), 32829–32843. doi: 10.1021/acsomega.5c01432
- Goyal, D., Shuaib, S., Mann, S., & Goyal, B. (2017). Rationally designed peptides and peptidomimetics as inhibitors of amyloid- β (A β) aggregation: potential therapeutics of Alzheimer's disease. *ACS Combinatorial Science*, *19*(2), 55-80. doi: 10.1021/acscombsci.6b00116
- Goyal, D., Kaur, A., & Goyal, B. (2018). Benzofuran and indole: promising scaffolds for drug development in Alzheimer's disease. *ChemMedChem*, *13*(13), 1275-1299. doi: 10.1002/cmdc.201800156
- Haroon, M., Khalid, M., Shahzadi, K., Akhtar, T., Saba, S., Rafique, J., ... Imran, M. (2021). Alkyl 2-(2-(arylidene) alkylhydrazinyl) thiazole-4carboxylates: Synthesis, acetyl cholinesterase inhibition and docking studies. *Journal of Molecular Structure*, 1245, 131063. doi: 10.1016/j. molstruc.2021.131063

- Hiremathad, A., Chand, K., Tolayan, L., Rajeshwari, Keri, R. S., Esteves, A. R.,... Santos, M. A. (2018a). Hydroxypyridinone-benzofuran hybrids with potential protective roles for Alzheimer's disease therapy. *Journal of Inorganic Biochemistry*, 179, 82-96. doi: 10.1016/j.jinorgbio.2017.11.015
- Hiremathad, A., Chand, K., & Keri, R. S. (2018b). Development of coumarin-benzofuran hybrids as versatile multitargeted compounds for the treatment of Alzheimer's disease. *Chemical Biology & Drug Design*, 92(2), 1497-1503. doi: 10.1111/cbdd.13316
- Irfan, A., Faisal, S., Ahmad, S., Al-Hussain, S. A., Javed, S., Zahoor, A. F., ... Zaki M. E. A. (2023a). Structure-based virtual screening of furan-1,3,4-oxadiazole tethered N-phenylacetamide derivatives as novel Class of hTYR and hTYRP1 inhibitors. *Pharmaceuticals*, 16, 344. doi: 10.3390/ph16030344
- Irfan, A., Faisal, S., Zahoor, A. F., Noreen, R., Hussain, S. A. Al-, Tuzun, B., ... Abdellattif M. H. (2023b).
 In silico development of novel benzofuran-1,3,4-oxadiazoles as lead inhibitors of m. tuberculosis polyketide synthase 13. *Pharmaceuticals*, 16(6), 829. doi: 10.3390/ph16060829
- Jehangir, U., Khan, S., Hussain, R., Khan, Y., Rahim, F., Iqbal, T., ... Alasmari A. F. (2024). In vitro and in silico correlation of bis-thiazole based Schiff base hybrids analogues: A computational approach develop to promising acetylcholinesterase and butyrylcholinesterase inhibitors. *Journal of Molecular Structure*, 1303, 137585. doi: 10.1016/j. molstruc.2024.137585
- Karakaya, A., Çevik, U. A., Erçetin, T., Özkay, Y., & Kaplancıklı, Z. A. (2023a). Synthesis of imidazole-thiazole derivatives as acetylcholinesterase and butyrylcholinesterase inhibitory activities. Pharmaceutical Chemistry Journal, 57(9), 1439-1443. doi: 10.1007/s11094-023-03007-8

- Karakaya, A., Maryam, Z., Ercetin, T., & Çevik, U. A. (2023b). Synthesis of thiazole derivatives as cholinesterase inhibitors with antioxidant activity. *European Journal of Life Sciences*, *2*(3), 118-124. doi: 10.55971/EJLS.1374823
- Karakaya, A., Ercetin, T., Yıldırım, S., Kocyigit, Ü. M., Rudrapal, M., Rakshit, G., ... Özkay, Y. (2024). New thiazole derivatives: carbonic anhydrase I–II and cholinesterase inhibition profiles, molecular docking studies. *Chemistry Select*, 9, e202401587. doi: 10.1002/slct.202401587
- Karrouch, K., Radi, S., Ramli, Y., Taoufik, J., Mabkhot,
 Y. N., Al-Aizari, F. A., & Ansar, M. H. (2018).
 Synthesis and pharmacological activities of pyrazole derivatives: a review. *Molecules*, 23(1), 134. doi: 10.3390/molecules23010134
- Kaya, B., Çevik, U. A., Karakaya, A., & Ercetin, T. (2024). Synthesis, anticholinesterase and antioxidant activity of thiosemicarbazone derivatives. *Cumhuriyet Science Journal*, 45(3), 519-523. doi: 10.17776/csj.1438171
- Kaya, B., Çevik, U. A., Behçet, M., Karayel, A., Daoud, N.E.-H., Bostancı, H. E., & Kaplancıklı, Z. A. (2025). Synthesis, antibacterial, anti-urease, DFT and molecular docking studies of novel bis-1,3,4thiadiazoles. *Journal of Molecular Structure*, 1321, 140134. doi: 10.1016/j.molstruc.2024.140134
- Kuzu, B., Alagoz, M. A., Demir, Y., Gulcin, I., Burmaoglu, S., & Algul, O. (2024). Structurebased inhibition of acetylcholinesterase and butyrylcholinesterase with 2-Aryl-6-carboxamide benzoxazole derivatives: synthesis, enzymatic assay, and in silico studies. *Molecular Diversity*, 29(1), 671–693.doi: 10.1007/s11030-024-10828-6
- Laczkowski, Z. K., Misiura, K., Biernasiuk, A., Malm, A., Siwek, A., & Plech, T. (2013). Synthesis, antimicrobial activities and molecular docking studies of novel 6-hydroxybenzofuran-3(2H)-one based 2,4-disubstituted 1,3-thiazoles. *Letters in Drug Design & Discovery*, 10(9), 798-807. doi: 10.2174/15701808113109990010.

- Li, G., Hong, G., Li, X., Zhang, Y., Xu, Z., Mao, L., ... Liu, T. (2018). Synthesis and activity towards Alzheimer's disease in vitro: Tacrine, phenolic acid and ligustrazine hybrids. European Journal of Medicinal Chemistry, 148, 238-254. doi: 10.1016/j. ejmech.2018.01.028
- Lipinski, C. A. (2004). Lead- and drug-like compounds: the rule-of-five revolution. *Drug Discovery Today: Technologies*, *1*(4), 337-341. doi: 10.1016/j.ddtec.2004.11.007
- Lipinski, C. A., Lombardo, F., Dominy, B. W., & Feeney, P. J. (2012). Experimental and computational approaches to estimate solubility and permeability in drug discovery and development settings. Advanced Drug Delivery Reviews, 64, 4-17. doi: 10.1016/j.addr.2012.09.019
- Loğoğlu, E., Yilmaz, M., Katircioğlu, H., Yakut, M., & Mercan, S. (2010). Synthesis and biological activity studies of furan derivatives. *Medicinal Chemistry Research*, 19(5), 490-497.
- Marucci, G., Buccioni, M., Ben, D. D., Lambertucci, C., Volpini, R., & Amenta, F. (2021). Efficacy of acetylcholinesterase inhibitors in Alzheimer's disease. *Neuropharmacology*, 190, 108352. doi: 10.1016/j.neuropharm.2020.108352
- Meng, X.-Y., Zhang, H.-X., Mezei, M., & Cui, M. (2011). Molecular docking: a powerful approach for structure-based drug discovery. Current Computer-Aided Drug Design, 7(2), 146-157. doi: 10.2174/157340911795677602
- Pravin, N., & Jozwiak, K. (2022). Effects of linkers and substitutions on multitarget directed ligands for Alzheimer's diseases: emerging paradigms and strategies. *International Journal of Molecular Sciences*, 23(11), 6085. doi: 10.3390/ijms23116085

- Patel, P., Shakya, R., Asati, V., Kurmi, B. D., Verma, S. K., Gupta, G. D., & Rajak, H. (2024). Furan and benzofuran derivatives as privileged scaffolds as anticancer agents: SAR and docking studies (2010 to till date). Journal of Molecular Structure, *1299*, 137098. doi: 10.1016/j.molstruc.2023.137098
- R. P. D. Bank, RCSB PDB 1EVE: Three Dimensional Structure Of The Anti-Alzheimer Drug, E2020 (Aricept), Complexed with Its Target Acetylcholinesterase, Resolution: 2.50 Å. 1999, https://www.rcsb.org/structure/1EVE
- R. P. D. Bank, RCSB PDB 4BDS: Human butyrylcholinesterase in complex with tacrine, Resolution: 2.10 Å. 2013, https://www.rcsb.org/ structure/4bds
- Ripain, I. H. A., & Ngah, N. (2021). A brief review on the thiazole derivatives: synthesis methods and biological activities. *Malaysian Journal of Analytical Sciences*, 25(2), 257-267. Retrieved from https://mjas.analis.com.my/
- Sahu, R., Shah, K., Misbah, A., Paliwal, D., Sharma, N., & Rani, T. (2024). Recent advancement of benzofuran in treatment of Alzheimer's disease. *Indian Journal of Pharmaceutical Sciences*, 85(6), 1539-1550. doi: 10.36468/pharmaceuticalsciences.1208
- Schrödinger L., Schrödinger Release 2021-2: 2021a. Maestro v12.8.117 In Schrödinger Inc.: New York, NY, USA www.schrodinger.com
- Schrödinger L., Schrödinger Release 2021-2: 2021b. LigPrep. In Schrödinger Inc.: New York, NY, USA www.schrodinger.com
- Schrödinger L., Schrödinger Release 2021b-2: 2021c. Protein Preparation Wizard Panel. In Schrödinger Inc.: New York, NY, USA www.schrodinger.com

- Schrödinger L., Schrödinger Release 2021-2: 2021d. Receptor Grid Generation Panel. In Schrödinger Inc.: New York, NY, USA www.schrodinger.com
- Schrödinger L., Schrödinger Release 2021-2: 2021e. Ligand Docking Panel. In Schrödinger Inc.: New York, NY, USA www.schrodinger.com
- Schrödinger L., L, Schrödinger Release 2021-2: 2021f. QikProp. In Schrödinger Inc.: New York, NY, USA www.schrodinger.com
- Schrödinger L., Schrödinger Release 2021-2: 2021g. Epik Panel. In Schrödinger Inc.: New York, NY, USA www.schrodinger.com
- Sepehri, S., Saeedi, M., Larijani, B., & Mahdavi, M. (2022). Recent developments in the design and synthesis of benzylpyridinium salts: Mimicking donepezil hydrochloride in the treatment of Alzheimer's disease. Frontiers in Chemistry, 10, 936240. doi: 10.3389/fchem.2022.936240
- Tran-Minh, C., Pandey, P., & Kumaran, S. (1999). Studies on acetylcholine sensor and its analytical application based on the inhibition of cholinesterase. *Biosensors and Bioelectronics*, *5*(6), 461-471. doi: 10.1016/0956-5663(90)80035-C
- Zhong, G., Guo, J., Pang, C., Su, D., Tang, C., Jing, L., ... Jiang, N. (2023). Novel AP2238-clorgiline hybrids as multi-target agents for the treatment of Alzheimer's disease: design, synthesis, and biological evaluation. *Bioorganic Chemistry*, 130, 106224. doi: 10.1016/j.bioorg.2022.106224
- Xu, Y., Jian, M. M., Han, C., Yang, K., Bai, L. G., Cao, F., & Ma, Z. Y. (2020). Design, synthesis and evaluation of new 4-arylthiazole-2-amine derivatives as acetylcholinesterase inhibitors. Bioorganic Medicinal Chemistry Letters, 30(6), 126985. doi: 10.1016/j.bmcl.2020.126985